Journal of Neuroscience Methods 352 (2021) 109081

Contents lists available at ScienceDirect

Journal of Neuroscience Methods

journal homepage: www.elsevier.com/locate/jneumeth

Quantitative determination of neuronal size and density using flow cytometry

L.F. Farrow [a], N.M Andronicos [b], P.G. McDonald [a], A.S. Hamlin [b,*]

[a] Animal Behaviour and Ecology Laboratory, School of Environmental and Rural Science, Faculty of Science, Agriculture, Business and Law, University of New England, Armidale, NSW, Australia

[b] Brain Behaviour Research Group, School of Science and Technology, Faculty of Science, Agriculture, Business and Law, University of New England, Armidale, NSW, Australia

ARTICLE INFO

Keywords:
Isotropic fractionator
Flow cytometry
High-throughput
Neuronal size
Neuronal density
Neuron glia ratios

ABSTRACT

Background: Recent anthropomorphic disturbances are occurring at an increasing rate leading to organisms facing a variety of challenges. This change is testing the information processing capacity (IPC) of all animals. Brain function is widely accepted to be influenced by a variety of factors, including relative size, number of neurons and neuronal densities. Therefore, in order to understand what drives an animals IPC, a methodological approach to analyze these factors must be established.

New method: Here we created a protocol that allowed for high-throughput, non-biased quantification of neuronal density and size across six regions of the brain. We used the Isotropic Fractionator method in combination with flow cytometry to identify neuronal and non-neuronal cells in the brains of adult rats.

Comparison with existing methods: The results obtained were comparable to those identified using stereological counting methods.

Results: By employing this new method, the number of nuclei in a specific brain region can be compared between replicate animals within an experiment. By calibrating the forward scatter channel of the flow cytometer with size standard beads, neuronal and non-neuronal nuclear sizes can be estimated simultaneously with nuclei enumeration. These techniques for nuclear counting and size estimation are technically and biologically reproducible.

Conclusion: Use of flow cytometry provides a methodological approach that allows for consistency in research, so that information on brain morphology, and subsequent function, will become comparable across taxa.

1. Introduction

Organisms face a variety of physical and cognitive challenges throughout their lives. Recently, anthropomorphic disturbances, including climate change, are occurring at an escalated rate (Thuiller et al., 2008). This increase in change and variability of conditions is testing the information processing capacity (IPC) of all animals (Sih et al., 2011), wherein working memory and mental manipulation will be key to survival at both the species and community level (Berg and Ellers, 2010). Consequently, an array of studies aim to identify the impact IPC has on a species ability to adapt to rapid changes, yet understanding why IPC varies across species remains controversial (Holekamp et al., 2013; Callaghan et al. 2019).

Brain function, and subsequently IPC, is widely accepted to be influenced by a variety of factors, including relative size (Sol et al., 2005; Deaner et al., 2007), number of neurons and neuronal densities (Dicke and Roth, 2016), glial to neuronal ratios (Herculano-Houzel, 2014) and potentially size of neuronal and non-neuronal cells (Herculano-Houzel and Lent, 2005). Therefore, in order to understand what drives an animals IPC, a methodological approach to analyze these factors must be established.

Originally, neuronal counts and densities were estimated using stereological methods, such as the optical dissector (Sterio, 1984), that were restricted to well-defined structures and measurable volumes (West, 1999). To account for these limitations Herculano-Houzel and Lent (2005) developed the Isotropic Fractionator (IF) method that allowed for semi-quantitative counts of neuronal and non-neuronal cells regardless of density. This method provided a reliable and reproducible

* Corresponding author.
E-mail address: ahamlin@une.edu.au (A.S. Hamlin).

https://doi.org/10.1016/j.jneumeth.2021.109081
Received 26 February 2020; Received in revised form 19 December 2020; Accepted 14 January 2021
Available online 20 January 2021

means of measuring total cell numbers across neuroanatomical regions. While successful, this approach is labor intensive and requires stereological counting. As such, Young et al. (2012) elaborated upon the IF method and employed flow cytometry cell counting technology to analyze the proportion of neurons in cortical regions of baboons (*Papio hamadryas Anubis*) that was analogous to the IF method employed by Herculano-Houzel and Lent (2005).

Flow cytometric technology enables the rapid analysis of single cells or particles (e.g. cell nuclei) as they flow past lasers while suspended in a buffered salt-based solution (McKinnon, 2018). Semi-quantitative parameters such as particle sizes (Forward Scatter, FSC) and granularity (Side Scatter, SSC) can be easily determined. The nuclei of cells are identifiable by staining the DNA with propidium iodide (PI), a red fluorescent dye (Deitch et al., 1982). Labeling of cells or particles with fluorescent antibodies and/or dyes enable identification of cells or particles in a complex solution. This method results in high-throughput cell population estimates allowing the creation of neuronal distribution maps. While these methods allow for semi-quantitative analysis of neuronal and non-neuronal cell counts, there is a need to understand the size and overall composition of these cells across brain regions and the brain overall.

Calibration of flow cytometers with beads of different sizes converts semi-quantitative forward scatter parameter into an absolute physical dimension. Thus, it is hypothesized that the number and size of cell nuclei within a tissue homogenate, spiked with enumeration beads can be efficiently quantified using a flow cytometer that has been calibrated with size beads. Therefore, the aim of this study was to define a reproducible, quantitative flow cytometric method for neuron and non-neuronal cell enumeration and characterization that minimizes errors associated with traditional semi-quantitative stereological techniques thereby increasing the throughput and reliability of acquired data obtained within a given sample. To achieve this, quantitative flow cytometric analysis of NeuN and PI labelled nuclei in homogenates isolated from the six anatomical regions of the brain were performed to determine the neuronal ($NeuN^+$) and non-neuronal ($NeuN^-$) nuclear (PI^+) densities and sizes in each region.

This method allows for intra-sample sampling to ensure repeatability of results, as well as an ability to compare regions within a given individual and across various specimens. It is anticipated that this methodological approach will thus make it possible to compare factors of the brain postulated to be responsible for variation in function (particularly IPC) across individuals of various ages and/or species.

2. Materials and methods

2.1. Animals

Experimentally naive male (n = 6) and female (n = 3) adult Wistar rats (10–12 weeks) (250–350 g) were obtained from The Centre for Research and Teaching, University of New England. The procedures were approved by the University of New England Animal Ethics Committee (AEC18-132) and conducted in accordance with the National Institutes of Health Guide for the Care and Use of Laboratory Animals (NIH Publications No. 8023) revised 1996. The procedures were designed to minimize the number of animals used and their suffering.

2.2. Tissue preparation and flow cytometric analysis

Rats were deeply anesthetized with sodium pentobarbital (100 mg/kg i.p.) and perfused transcardially with 100 mL of 0.9 % saline, containing 1.25 mL 1 % sodium nitrite and 0.036 mL heparin sodium (5000 i.u./mL), followed by 500 mL of 4 % paraformaldehyde in 0.1 M phosphate buffer (PB), pH 7.4. Brains were dissected and post-fixed for 1 h in the same fixative before being placed in 1% NaN_3 in 0.1 M PBS for a minimum of three days. Each brain was weighed (whole brain post-fixative weight) and mid-sagittally hemisected. The brain was then micro dissected into the regions identified by (Olkowicz et al., 2016); tectum, cerebellum, cortex, forebrain, brain stem and the diencephalon (Fig. 1).

Once dissected, the regions were weighed before being placed into 1.5 mL microfuge tubes containing 1 mL homogenization buffer (40 mM sodium citrate buffer (pH 6.0) with 1 % Triton X-100 (Herculano-Houzel and Lent, 2005) The tissue was then placed in a glass dounce homogenizer (Kontes glass company tube rod = C35, USA) and homogenized for 60 s to form an isotropic suspension of cell debris including nuclei. To further reduce between sample artefacts in the sample, the isotropic suspension was then filtered through a 30 μm pre-separation filter (Miltenyi Biotec, USA) placed directly over a 15 mL centrifuge tube. The 30 μm filter was washed with an additional 1 mL of homogenization buffer to quantitatively collect the nuclei in the filtrate and 100 μL samples of the isotropic suspension were placed into microfuge tubes and centrifuged at 300 *g* for 3 min at room temperature. An additional 100 μL sample of the isotropic suspension for each brain region was collected (n = 4) for biological replication. The supernatant was discarded, and the pellet resuspended in 100 μL of homogenization buffer containing a 1:100 dilution of mouse anti-NeuN monoclonal antibody (EMD Millipore, USA) or isotype control antibody (EMD Millipore, USA) for 30 min on ice.

The brain tissue lysate was washed by adding 1 mL of ice-cold PBS (pH 7.4) and centrifuged at 300 g for 3 minutes and the supernatant discarded. The pellets were resuspended in 100 μl of homogenization buffer containing a 1:200 dilution of goat anti-mouse IgG-FITC antibody (EMD Millipore, USA) for 30 minutes on ice in the dark. Brain tissue lysate was washed by adding 1 ml of PBS (pH7.4) and centrifuged at 300 g for 3 minutes. The supernatant was discarded and the cells resuspended in 100 μl of PBS (pH 7.4) and were stored on ice in the dark.

Just prior to flow cytometric acquisition, 1 μL of 1 mg/mL propidium iodide (PI) was added to each sample, along with 50 μL of precision count beads (Biolegend, USA). The sample tubes were inverted six times to homogenously mix the beads and PI stained nuclei. Flow cytometric data were acquired using a FlowSight imaging flow cytometer (Merck, USA). Data acquisition was completed for each sample when the number of events in the single bead counting gate reached 500. This process was repeated twice for four individual samples for each brain region for technical replication. To quantify nuclear size the forward scatter (FSC) scale of the flow cytometer was converted into microns via the acquisition of size calibration beads (1–15 μm; Thermoscientific, USA) using the same cytometer settings.

2.3. Statistical analysis

Statistical analyses of flow cytometric data were performed using the

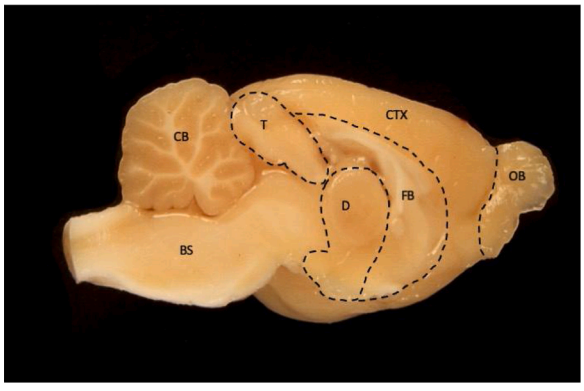

Fig. 1. Dissected regions of rat brain for flow cytometric analysis. Midsagittal section of the rat brain showing regions dissected for flow cytometric analysis. Tectum (T), cerebellum (CB), cortex (CTX), forebrain (FB), brain stem (BS), diencephalon (D) and the optic bulb (OB).

SPSS statistical analysis package, version 25 (IBM, USA). For flow cytometric data analysis only single particle events were analysed. Neuronal nuclei (PI^+NeuN^+) and non-neuronal nuclei (PI^+NeuN^-) were gated and the size distribution determined relative to the FSC (mean ± SD) of the size calibration beads for each brain region. For the multivariate comparison of neuronal and non-neuronal nuclei in the various brain regions the Box's Test of Equality of Covariance Matrices was not significant ($p = 0.214$), therefore linear regression ANOVA with Tukey's post-hoc tests were used as the tests of significance. The significance of neuronal nuclear size distribution was determined by Kruskal-Wallis test for each brain region as these data were not normally distributed. The distribution of non-neuronal cell nuclei and neuronal nuclei had a skewed distribution, therefore, to determine significant differences of the neuronal nuclei to non-neuronal nuclei for the various brain regions Mann-Whitney U tests were performed. For all statistical tests of significance, a p-value < 0.05 was deemed significant.

3. Results

3.1. Flow cytometric gating strategy and reproducibility

Fig. 2 describes the flow cytometric gating strategy used to quantify the size and number of neuronal (PI^+NeuN^+) and non-neuronal (PI^+NeuN^-) nuclei in various regions of the rat brain. Only single particle signals were used to generate flow cytometric data (Fig. 2A). A scatter plot of FSC against PI fluorescence intensity of the single particle cell debris was plotted to identify (gate) the population of single nuclei (PI^+ particles; Fig. 2B). By only analyzing single particles there was a clear demarcation between the spiked enumeration beads and particles in the homogenate. Histograms of PI^+ nuclei stained with either NeuN antibody to identify neuronal nuclei or an irrelevant isotype control antibody were used to define the $NeuN^+$ nuclei gate relative to the isotype control ($NeuN^-$) signal (Fig. 2C). The FSC against NeuN fluorescence intensity scatter plot of PI^+ particles (nuclei; Fig. 2D) were used to differentiate between neuronal and non-neuronal nuclei and demonstrated that PI^+NeuN^+ neuronal nuclei had a greater size distribution than PI^+NeuN^- non-neuronal nuclei. Once neuronal and non-nuclei populations were defined, histograms of the non-neuronal nuclei (PI^+NeuN^-) and neuronal nuclei (PI^+NeuN^+; Fig. 2F) were plotted and superimposed with bead size (mean FSC ± 1 SD; from Fig. 2E) calibration gates to determine the number of nuclei within each size gate, thereby quantifying the non-neuronal (PI^+NeuN^-) and neuronal (PI^+NeuN^+) nuclei sizes in the respective homogenates from the various anatomical locations of the brain. Thus, the gating strategy used, facilitated the identification of nuclei within the cell debris which enabled the quantitation of neuronal and non-neuronal nuclear sizes and numbers in the different regions of the rat brain by two methods. First, overlaying bead size FSC gates (mean FSC ± 1 SD; Fig. 2E) on to Fig. 2F

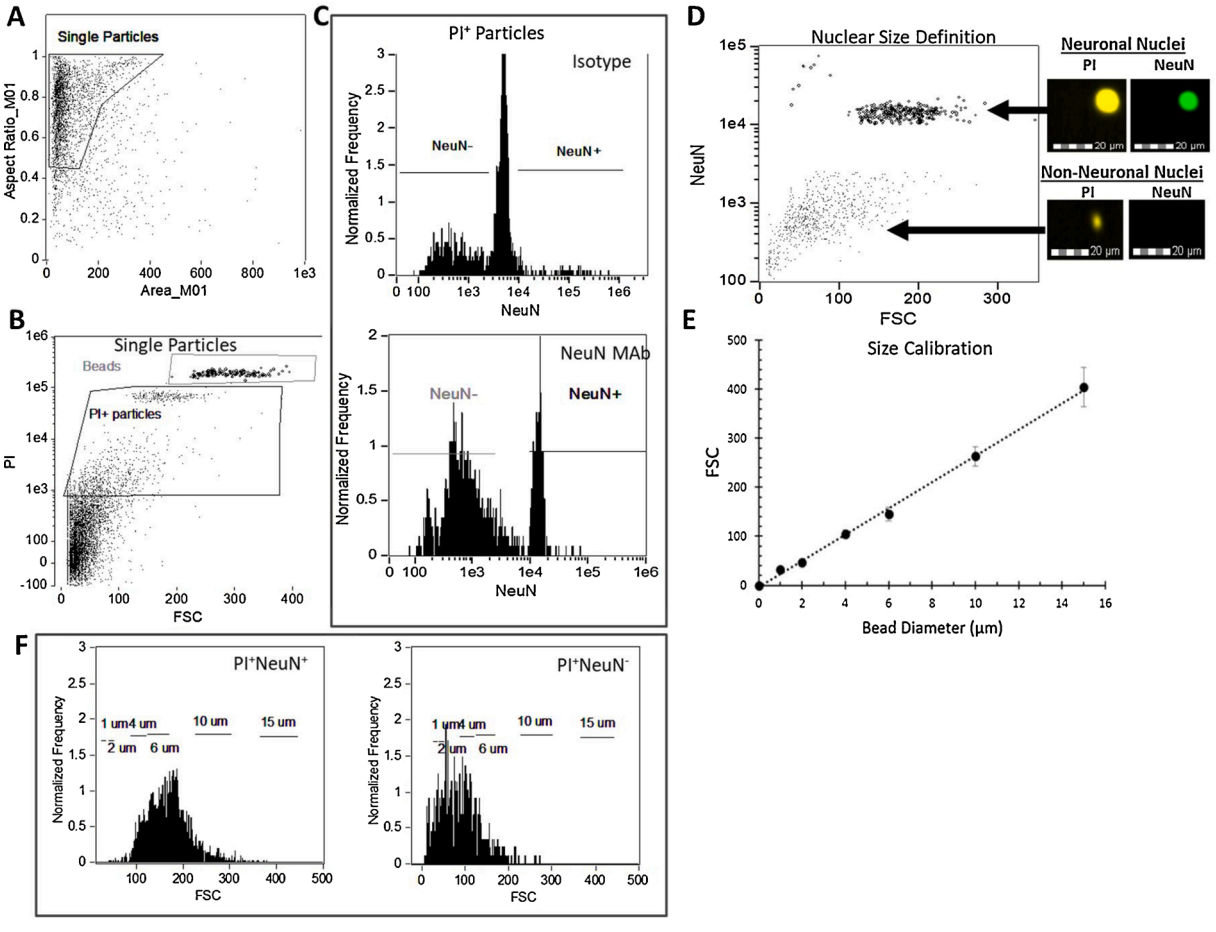

Fig. 2. Imaging flow cytometric gating strategy. (A) A scatter plot of Area against Aspect Ratio to define single particles within the brain tissue homogenates. (B) A scatter plot of single particles of forward scatter (FSC) against propidium iodide (PI) fluorescent intensity used to define the PI^+ nuclei in the cell debris. (C) NeuN channel intensity histograms of brain homogenates stained with either NeuN antibody or an irrelevant isotype control antibody. (D) FSC against NeuN scatter plot of the PI^+ nuclei population from (B) used to define neuronal (PI^+NeuN^+) and non-neuronal (PI^+NeuN^-) nuclei populations using $NeuN^+$ and $NeuN^-$ gates defined in (C) as well as flow cytometric micrographs defining the staining pattern of neuronal and non-neuronal nuclei. (E) Bead dimensions against FSC for the size calibration beads (1 to 15 µm). (F). Histograms of PI^+NeuN^- non-neuronal nuclei and PI^+NeuN^+ neuronal nuclei with superimposed bead size (median ± SD from (E)) calibration gates.

histograms or second, by using the equation from the bead diameter against FSC standard curve (Fig. 2E) to calculate the physical size from the FSC of each particle from Fig. 2F.

The reproducibility of the nuclei sampling technique employed was determined (Fig. 3). Homogenates from different brain regions were stained with PI and NeuN, spiked with enumeration beads and acquired on the flow cytometer. The gating strategy described in Fig. 2 was used for all technical replicate comparisons. Overall, there was a significant ($p = 0.001$) difference between technical replicates. As expected, the variation between different anatomical regions of the brain was responsible for the significant ($p = 0.002$) difference observed for the total technical replicate variation. In contrast, there were no significant differences between technical replicates when nuclei type or antibody stain parameters. However, nuclear sizes between 4 and 6 μm had greater, but non-significant variability between technical replicates. Collectively these data suggested that the reproducibility of this flow cytometric technique for nuclei size and enumeration was adequate.

3.2. Quantitative flow cytometric nuclei count analysis

The first step in defining the neuronal density of various anatomical regions of the rat brain was to quantify total neuronal (PI^+NeuN^+) and non-neuronal (PI^+NeuN^-) nuclei in the homogenates using quantitative flow cytometry (Fig. 4). The quantitative acquisition of nuclei in brain homogenates were standardized via the addition of a known quantity of enumeration beads and creating a stopping gate when a set number of beads had been acquired. In the brain stem, cortex, diencephalon, forebrain and tectum regions of the rat brain there were significantly ($p = 1.2 \times 10^{-28}$) more (6–22 fold) non-neuronal nuclei (PI^+NeuN^-) compared to neuronal nuclei (PI^+NeuN^+; Fig. 4). In contrast, the numbers of non-neuronal (PI^+NeuN^-) and neuronal (PI^+NeuN^+) nuclei in the cerebellum were not significantly different (Fig. 4).

3.3. Quantitative flow cytometric nuclei count analysis

Two methods for determining nuclear sizes from the flow cytometric FSC data were evaluated. First, neuronal and non-neuronal nuclear sizes were stratified by overlaying the FSC parameter for each bead size plus/minus one standard deviation as gates on the PI^+NeuN^+ (neuronal) and PI^+NeuN^- (non-neuronal) nuclei FSC histograms (Fig. 2F). For this analysis the size by nuclear type varied significantly ($p = 4.7 \times 10^{-51}$)

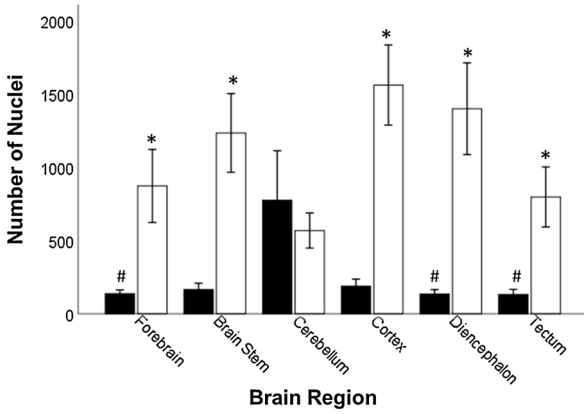

Fig. 4. Total number of neuronal (PI^+NeuN^+;■) and non-neuronal (PI^+NeuN^-; □) nuclei in the different anatomical regions of the rat brain as determined by quantitative flow cytometric analysis. * $p < 0.05$ non-neuronal nuclei compared to neuronal nuclei numbers. # $p < 0.05$ for neuronal nuclei comparisons across brain regions.

and accounted for 18.2 % of the total variation. Fig. 5 demonstrated that quantitative flow cytometric analysis of neuronal nuclear size indicated that there were significant ($p < 0.05$) enrichments of neuronal nuclear sizes between 6–10 μm in the brain stem, cortex and the diencephalon regions of the brain when compared to 1 μm neuronal nuclei (Fig. 5). Similarly, there was a significant enrichment of 4–10 μm neuronal nuclei in the forebrain and tectum regions of the rat brain compared to 1 μm neuronal nuclei. Finally, the cerebellum contained a more homogenous neuronal nuclei composition with 6 μm nuclei being significantly enriched relative to 1 μm nuclei.

In contrast, non-neuronal nuclei had smaller nuclear sizes than neuronal nuclei (Fig. 5). Specifically, there were significantly more 1 and 2 μm non-neuronal nuclei in all the brain regions compared to neuronal nuclei.

The second nuclear size analysis method involved using the equation defined by the bead size against FSC standard curve (Fig. 2E) to convert FSC data into micron dimensions for each PI^+ particle (Fig. 6). The bead size calibration standard curve enabled the estimation of nuclei numbers per micron from 1 to 14 μm and demonstrated that neuronal nuclear sizes were normally distributed for the cerebellum, cortex, diencephalon

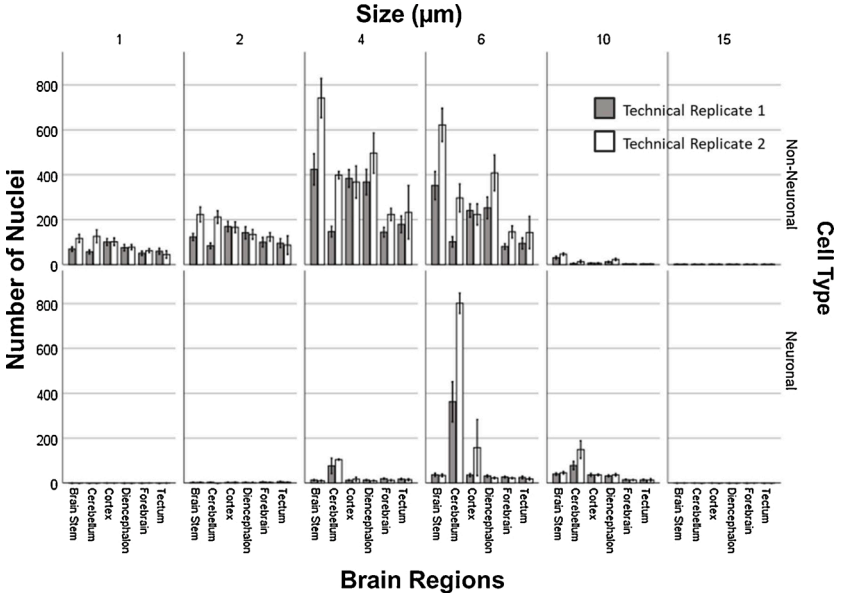

Fig. 3. Reproducibility of sizes of neuronal and non-neuronal nuclei for the various regions of the rat brain.

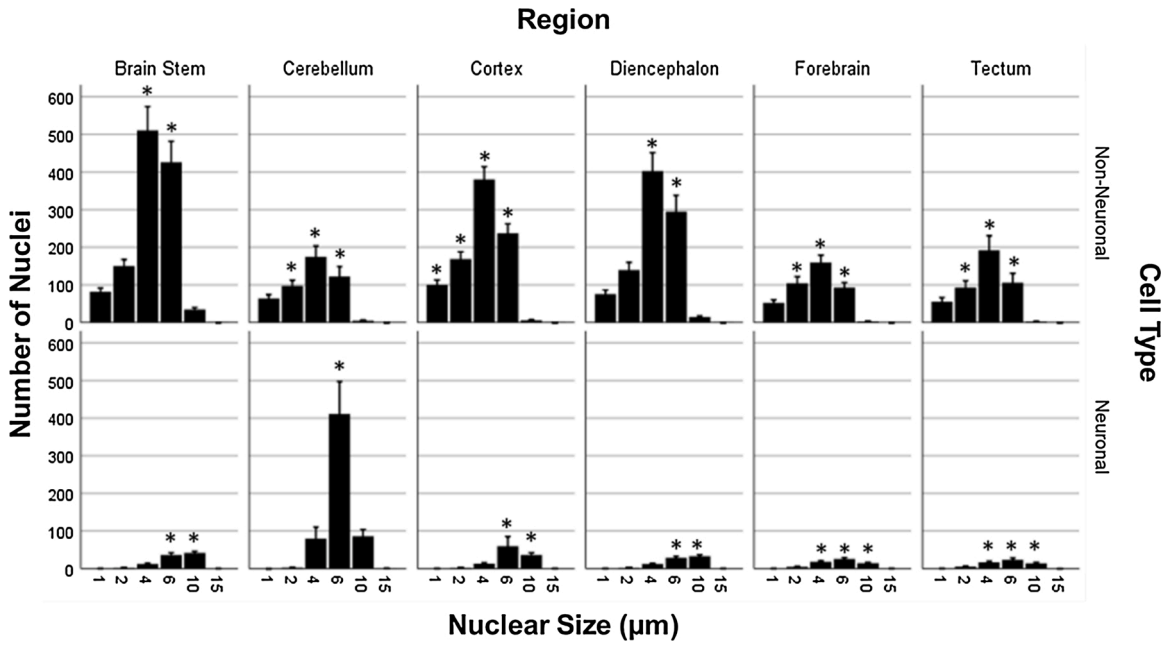

Fig. 5. Nuclear size distribution of neuronal (PI^+NeuN^+) and non-neuronal (PI^+NeuN^-) nuclei defined using the FSC ± 1 SD for each size calibration bead overlaid as gates onto each of the PI^+NeuN^+ and PI^+NeuN^- histograms. $p < 0.05$ for neuronal nuclear sizes relative 1 µm neuronal nuclei and $p < 0.05$ for non-neuronal nuclear sizes relative 10 µm non-neuronal nuclei.

and brain stem having 6.6, 7.1, 7.0 and 7.3 µm as their average nuclear sizes, respectively, whereas the forebrain and tectum had smaller neuronal nuclear sizes with mean nuclear size of 6.0 and 5.8 µm, respectively. In contrast, smaller non-neuronal nuclei were present in these same anatomical regions but demonstrated a skewed size distribution and demonstrated a clear reduction in the number of non-neuronal nuclear sizes greater than at 4 µm for each region other than the tectum (data not shown). However, the number of non-neuronal nuclei estimated using the standard curve method were approximately 2 orders of magnitude above the estimates using the histogram gating method (data not shown).

3.4. Neuronal to non-neuronal ratios

The non-neuronal to neuron densities for each brain region were calculated by combining flow cytometric nuclear estimates with the tissue weight of anatomical brain regions (Table 1). Non-neuronal: neuronal ratios for the anatomical regions of the brain ranged from 0.8:1 in the cerebellum up to 13.5:1 in the diencephalon. The average non-neuronal: neuronal ratio across all the studied brain anatomical regions was estimated at 7.5:1 ± 4.10.

4. Discussion

Quantitative flow cytometric determination of cell nuclei numbers and sizes has several advantages over microscopy-based nuclei enumeration methods, including higher sample throughput and reproducibility. However, before flow cytometry can be used for determining cell nuclei number and sizes two criteria must be satisfied: First, only single particles should be analyzed. Second, semi-quantitative flow cytometric data must be converted into quantitative data by calibration of the flow cytometer with counting and size beads. These beads are readily available from numerous biotech supply companies. To identify nuclear material in the brain region homogenates the DNA were labelled with PI. Neuronal nuclei in these brain homogenates also expressed NeuN antigen (i.e. PI^+ $NeuN^+$). These labelled samples were spiked with a set volume of cell counting beads and acquisition of data from the homogenates stopped when a pre-defined target number of beads (500) in each sample was detected by the bead gate of the flow cytometer. By employing this method, the number of nuclei in a specific brain region could be compared between replicate animals within an experiment. In addition, by calibrating the FSC channel of the flow cytometer with size standard beads, neuronal and non-neuronal nuclear sizes could be estimated simultaneously with nuclei enumeration. These techniques for nuclear counting and size estimation were technically and biologically reproducible.

For nuclear size determination there were two possible methods for estimating nuclear size stratification. First, overlaying the neuronal and non-neuronal histograms with the FSC of bead sizes plus/minus one standard deviation. This analysis method provided data similar to previous studies (Sterio, 1984; Herculano-Houzel and Lent, 2005; Young et al., 2012) because only nuclear sizes that were within a single standard deviation were considered thereby reducing overestimation errors. An alternative analytical method to stratify nuclear sizes is to define the equation for the FSC bead calibration curve and use this equation to convert FSC of PI + NeuN+ (neuronal) and PI + NeuN- (non-neuronal) nuclei into physical sizes. The equation-based stratification method was comparable to the nuclear size overlay method for neuronal nuclei. However, for non-neuronal nuclei the equation-based method was too sensitive and resulted in a massive overestimation of non-nuclear material that were PI^+. Possible reasons for this discrepancy in nuclear estimates between the two calculation techniques may be DNA cross contamination. For example, neuronal nuclei were identified by the presence of PI and the nuclear antigen NeuN. Thus, NeuN antigen differentiated neuronal nuclei from PI + non-neuronal signals, which may be composed of non-neuronal nuclei, organelles with extra-nuclear DNA such as mitochondria or free DNA in the homogenate non-specifically binding to non-nuclear material. To improve the estimation of the non-neuronal content of specific brain regions nuclear markers for glial cells and vascular cells for example are required. Digestion of homogenates with DNase to reduce extranuclear DNA contamination may provide short term improvements to the accuracy of non-neuronal counts. Therefore, the current histogram overlay size gate method was preferred over the size standard equation estimation method because the PI^+ particles included in the estimation were within 1 standard deviation of the FCS of the bead, thereby reducing error. In

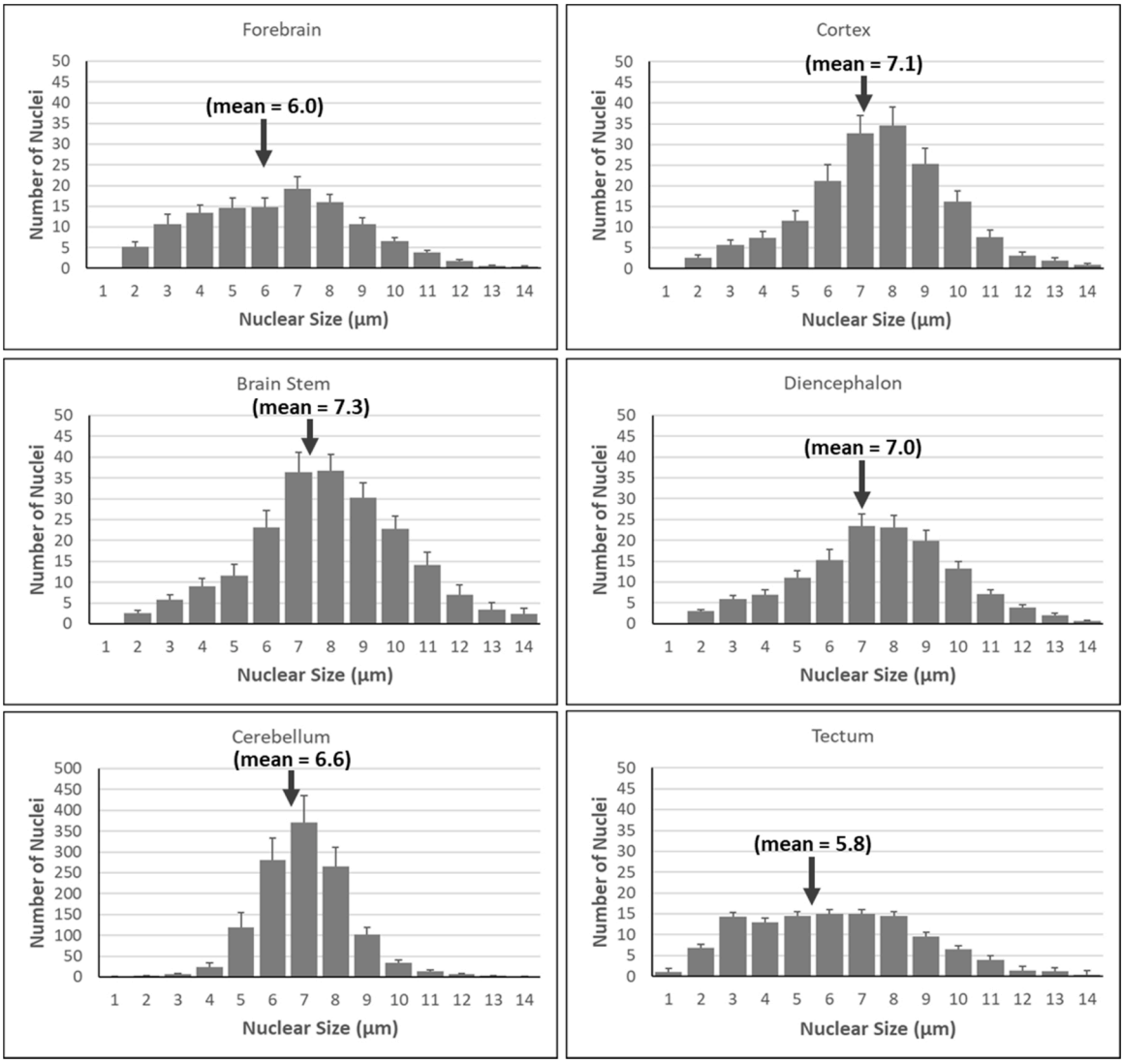

Fig. 6. Estimates of neuronal nuclear size distributions in various brain anatomical regions using the standard curve estimation method.

Table 1
Average weights (g) of brain regions and the mean non-neuronal and neuronal densities expressed as a ratio of flow cytometric nuclei counts per brain tissue weight (cells/g).

Brain Region	Tissue Weight (g)	[a]Non-Neuronal Density (10^4 cells/g)	[a]Neuronal Density (10^4 cells/g)	Non-Neuronal: Neuronal
Cortex	0.44 ± 0.009	8.2[#] ± 0.9870	0.94[*] ± 0.1976	8.7:1
Forebrain	0.050 ± 0.01	71.4 ± 24.644	8.74 ± 1.858	8.1:1
Diencephalon	0.08 ± 0.012	44.9 ± 13.211	3.33 ± 0.4096	13.5:1
Tectum	0.03 ± 0.002	55.0 ± 12.918	8.74 ± 1.773	6.3:1
Cerebellum	0.14 ± 0.006	87.1[#] ± 2.040	10.84 ± 3.923	0.8:1
Brain Stem	0.13 ± 0.006	19.3 ± 3.965	2.53 ± 0.6598	7.6:1

[a] The flow cytometric nuclei count data used to calculate the PI^+NeuN^- (non-neuronal) and PI^+NeuN^+ (neuronal) nuclei densities were derived from the total nuclei count data of the PI^+NeuN^- and PI^+NeuN^+ histograms (Fig. 2F), respectively for each anatomical brain region. n = 8; means ± SEM.

[*] $p < 0.05$ relative to the cerebellum neuronal nuclei density. # $p < 0.05$ relative to the forebrain.

contrast, sizes estimated using the equation-based method were rounded to the nearest whole micron. The limitation with the gating overlay method is that nuclear sizes may be under-estimated. For example, 3, 5, 7, 8, 9, 11, 12, 13 and 14 µm sizes were not estimated using this method.

The methodology described herein allowed for identification of a significant difference in the number of neurons present across the six regions dissected. Primarily, the cerebellum contained significantly more neurons than the forebrain, cortex, brain stem, diencephalon and tectum. These results are comparable to previous studies, in particular Herculano-Houzel and Lent (2005) that developed the isotropic fractionator (IF) using stereological counting methods that are more time-consuming and capture less events.

Previous research has stated that glial cells are more prominent than neuronal cells in the brain (Allen and Barres, 2009). This is the result of glia playing a crucial role in metabolic support for neurons (Sherwood et al., 2006) and control of synaptic formation (Ullian et al., 2001). While this was seen in the majority of brain regions analyzed in this study the cerebellum was an exception in that it offered a near 1:1 non-neuronal to neural nuclei ratio, possibly as a result of the neuronal density of granule cells in the cerebellum. However further research is required to investigate this potential link.

The original method of IF (Herculano-Houzel and Lent, 2005) identified the main disadvantage of IF as the inability to identify cell composition as the very nature of homogenization is to destroy the brain tissue. However, here, through overlay of size calibration bead gates onto PI^+NeuN^+ and PI^+NeuN^- FSC histograms, we were able to identify nuclear sizes (and density of these various sizes) across the six brain regions analyzed.

In conclusion, we have demonstrated a novel method of using IF to obtain accurate estimates of neuron sizes and density, across major regions of the brain, rapidly and with minimum opportunity for human error that is potentially applicable across a range of taxa. Further, it is anticipated that in creating a methodology that is concise and obtainable for many laboratories that have access to a flow cytometer, future results regarding brain morphology across taxa will be comparable. This in turn, would help shed some forward scatter light onto what makes a brain intelligent.

Ethical standards

The authors certify that these experiments were carried out in accordance with the National Institute of Health Guide for the Care and Use of Laboratory Animals (NIH Publications No. 80-23) revised 1996 or the UK Animals (Scientific Procedures) Act 1986 and associated guidelines, or the European Communities Council Directive of 24 November 1986 (86/609/EEC). The authors also certify that formal approval to conduct the experiments described has been obtained from the animal subjects review board of their institution and could be provided upon request. The authors further attest that all efforts were made to minimize the number of animals used and their suffering.

CRediT authorship contribution statement

L.F. Farrow: Conceptualization, Methodology, Validation, Formal analysis, Investigation, Writing - original draft, Writing - review & editing, Visualization, Funding acquisition. **N.M Andronicos:** Conceptualization, Methodology, Validation, Formal analysis, Investigation, Writing - review & editing, Visualization. **P.G. McDonald:** Supervision, Funding acquisition, Writing - review & editing. **A.S. Hamlin:** Conceptualization, Methodology, Validation, Formal analysis, Investigation, Writing - review & editing, Visualization, Resources, Data curation.

Declaration of Competing Interest

None.

Acknowledgements

This project was funded partially by the Holsworth Wildlife Research Endowment – Equity Trustees Charitable Foundation & the Ecological Society of Australia (Awarded to LF) and internal PhD research funding from the University of New England (to LF).

References

Allen, N.J., Barres, B.A., 2009. Glia — more than just brain glue. Nature 457 (7230), 675–677.
Berg, M.P., Ellers, J., 2010. Trait plasticity in species interactions: a driving force of community dynamics. Evol. Ecol. 24 (3), 617–629.
Callaghan, C.T., Major, R.E., Wilshire, J.H., Martin, J.M., Kingsford, R.T., Cornwell, W. K., 2019. Generalists are the most urban-tolerant of birds: a phylogenetically controlled analysis of ecological and life history traits using a novel continuous measure of bird responses to urbanization. Oikos 128 (6), 845–858.
Deaner, R.O., Isler, K., Burkart, J., Van Schaik, C., 2007. Overall brain size, and not encephalization quotient, best predicts cognitive ability across non-human primates. Brain Behav. Evol. 70 (2), 115–124.
Deitch, A.D., Law, H., deVere White, R., 1982. A stable propidium iodide staining procedure for flow cytometry. J. Histochem. Cytochem. 30 (9), 967–972.
Dicke, U., Roth, G., 2016. Neuronal factors determining high intelligence. Philos. Trans. Biol. Sci. 371 (1685), 20150180.
Herculano-Houzel, S., Lent, R., 2005. Isotropic fractionator: a simple, rapid method for the quantification of total cell and neuron numbers in the brain. J. Neurosci. 25 (10), 2518–2521.
Herculano-Houzel, S., 2014. The glia/neuron ratio: how it varies uniformly across brain structures and species and what that means for brain physiology and evolution. Glia 62 (9), 1377–1391.
Holekamp, K.E., Swanson, E.M., Van Meter, P.E., 2013. Developmental constraints on behavioural flexibility. Philos. Trans. R. Soc. Lond., B, Biol. Sci. 368 (1618), 20120350.
McKinnon, K.M., 2018. Flow cytometry: an overview. Curr. Protoc. Immunol. 120, 5.1.1-5.1.11.
Olkowicz, S., Kocourek, M., Lučan, R.K., Porteš, M., Fitch, W.T., Herculano-Houzel, S., Němec, P., 2016. Birds have primate-like numbers of neurons in the forebrain. Proc. Natl. Acad. Sci. U. S. A. 113 (26), 7255–7260.
Sherwood, C., Stimpson, C., Raghanti, M., Wildman, D., 2006. Evolution of increased glia-neuron ratios in the human frontal cortex. Proc. Natl. Acad. Sci. U. S. A. 103 (37), 13606.
Sih, A., Ferrari, M.C., Harris, D.J., 2011. Evolution and behavioural responses to human-induced rapid environmental change. Evol. Appl. 4 (2), 367–387.
Sol, D., Duncan, R.P., Blackburn, T.M., Cassey, P., Lefebvre, L., 2005. Big brains, enhanced cognition, and response of birds to novel environments. Proc. Natl. Acad. Sci. U. S. A. 102 (15), 5460–5465.
Sterio, D.C., 1984. The unbiased estimation of number and sizes of arbitrary particles using the disector. J. Microsc. 134 (Pt 2), 127–136.
Thuiller, W., Albert, C., Araujo, M.B., Berry, P.M., Cabeza, M., Guisan, A., Hickler, T., Midgely, G.F., Paterson, J., Schurr, F.M., Sykes, M.T., Zimmermann, N.E., 2008. Predicting global change impacts on plant species' distributions: future challenges. Perspect. Plant Ecol. Evol. Syst. 9 (3-4), 137–152.
Ullian, E., Sapperstein, S., Christopherson, K., Barres, B., 2001. Control of synapse number by glia. Science 291 (5504), 657–661.
West, M.J., 1999. Stereological methods for estimating the total number of neurons and synapses: issues of precision and bias. Trends Neurosci. 22 (2), 51–61.
Young, N.A., Flaherty, D.K., Airey, D.C., Varlan, P., Aworunse, F., Kaas, J.H., Collins, C. E., 2012. Use of flow cytometry for high-throughput cell population estimates in brain tissue. Front. Neuroanat. 6, 27.